The Effects of Acyl Chain Length and Saturation of Diacylglycerols and Phosphatidylcholines on Membrane Monolayer Curvature

Joseph A. Szule, Nola L. Fuller, and R. Peter Rand
Biological Sciences, Brock University, St. Catharines, Ontario L2S 3A1, Canada

ABSTRACT The second messenger, diacylglycerol (DAG), introduces negative curvature in phospholipid monolayers and strongly induces the lamellar (L_α) to reverse hexagonal (H_{II}) phase transition. The chain lengths and degree of unsaturation of symmetric DAGs influence this effect. Within dioleoylphosphatidylcholine (DOPC) monolayers, the apparent spontaneous radius of curvature (R_0) of the short, saturated dicaprylglycerol (C10-DCG) itself was determined to be −13.3 Å, compared with an R_0 value of −10.1 Å for the long, di-monounsaturated dioleoylglycerol (C18-DOG). Such increased length and unsaturation of the DAG acyl chains produces this small change. Di-saturated phosphatidylcholines (PCs) with equal length chains (from C10-C18) with 25 mol % DOG do not form the H_{II} phase, even under the unstressed conditions of excess water and alkane. Di-unsaturated PCs with equal chain length (from C14-C18) with 25 mol % DOG do form the H_{II} phase. Asymmetric chained PCs (position 1 saturated with varying lengths, position 2 differentially unsaturated with varying lengths) all form the H_{II} phase in the presence of 25 mol % DOG. As a general rule for PCs, their unsaturation is critical for the induction of the H_{II} phase by DOG. The degree of curvature stress induced by the second messenger DOG in membranes, and any protein that might be affected by it, would appear to depend on chain unsaturation of neighboring PCs.

INTRODUCTION

Some functions of biological membranes appear to be dependent on the localized spontaneous curvature of their constituent monolayers, particularly through the curvature contributions of the individual components. In isolation, many membrane lipids form non-bilayer structures (Luzzati and Husson, 1962). Cullis and de Kruijff (1979) attributed phase structure to "molecular shape." Helfrich (1973) and Gruner (1985) proposed the idea of spontaneous curvature ($1/R_0$), where R_0 is defined as the radius of monolayer curvature that minimizes the bending elastic free energy and is a property of the individual lipid species. Thus "cylindrical lipids" with zero curvature form flat lamellar L_α phases (i.e., phosphatidylcholines (PCs)). "Conical lipids" with relatively small polar groups and therefore negative curvature induce or form the reverse hexagonal H_{II} phase (e.g., phosphatidylethanolamines (PEs)), while "conical lipids" with large polar groups and positive curvature form either micelles or the hexagonal H_I phase (e.g., lysolipids). The lipid assemblies and the structural parameters of the lamellar and the reverse hexagonal H_{II} phases are shown in Fig. 1. The idea of spontaneous curvature implies that lipids contribute curvature stresses to flat biological membrane monolayers. Lipids that are prone to forming non-bilayer structures are believed to be important in membrane fusion (Chernomordik et al., 1995) and to modulate the activity of many membrane-associated enzymes. Various excellent reviews are collected in *Lipid Polymorphism and Membrane Properties* (Epand, 1997).

Various models of membrane fusion, including the stalk-pore hypothesis (for a review see Chernomordik et al. (1995)), involve highly curved structural intermediates. That these are likely composed of non-bilayer forming lipids is supported by the fact that the propensity for membrane fusion increases in the presence of non-bilayer-prone lipids (Ortiz et al., 1992; Siegel et al., 1989). An asymmetric transbilayer distribution of lipids has been shown experimentally (Verkleij et al., 1973; Rothman and Lenard, 1977). Asymmetry is an important part of the stalk-pore hypothesis, in which each monolayer of the fusing bilayers has opposite curvature requirements that affect fusion efficiency.

Acyl chain composition has previously been investigated in regard to membrane fusion. Roos and Choppin (1985a, b) have shown that the acyl chains of fusion-resistant cell membranes have decreased levels of polyunsaturation compared to fusion susceptible cells. It was hypothesized that the physicochemical properties (i.e., spontaneous curvature) associated with these differences in acyl chain composition affect membrane fusion.

Protein kinase C (PKC) is preferentially activated by naturally occurring diacylglycerols (DAGs) (Go et al., 1987; Mori et al., 1982) and DAGs with at least one unsaturated acyl chain (Nishizuka, 1984). DAGs with certain n-3 and n-6 polyunsaturated acyl chains were found to be even more effective activators (Marignani et al., 1996). The acyl chain unsaturation of neighboring phospholipids also affects PKC activation. Ca^{2+}/DAG-induced PKC activation was tested in saturated and unsaturated phosphatidylserine/phosphatidylcholine vesicles, and it was determined that phospholipid unsaturation was also required for PKC activation (Bolen and Sando, 1992).

Submitted November 2, 2001, and accepted for publication January 24, 2002.

Address reprint requests to Nola L. Fuller, 500 Glenridge Ave., St. Catharines, Ontario L2S 3A1, Canada. Tel.: 905-688-5550; Fax: 905-688-1855; E-mail: nfuller@brocku.ca.

0006-3495/02/08/977/08 $2.00

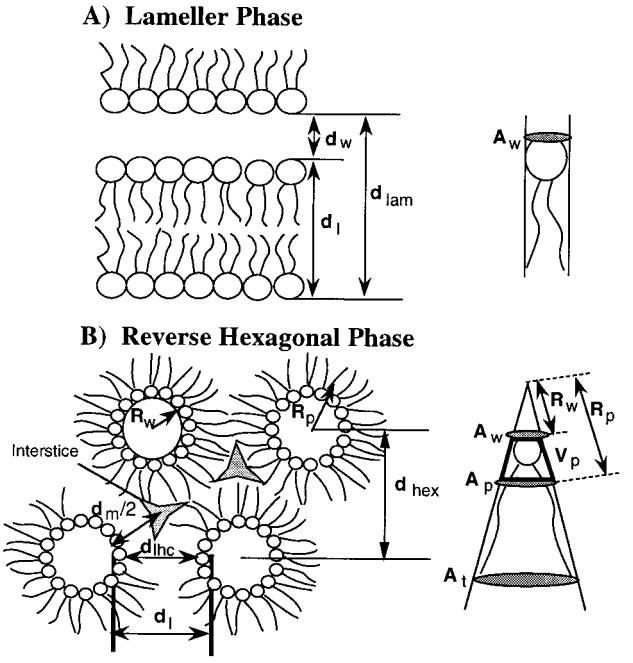

FIGURE 1 Schematic diagrams with structural parameters of (*A*) the lamellar and (*B*) the reverse hexagonal phase.

The functional roles of high-curvature lipids within a membrane do not usually involve the formation of non-bilayer structures, but likely involve the changes they produce in the physicochemical properties of the membrane. For example, curvature stresses induced by these non-bilayer-prone lipids affect the curvature energy of the bilayer, which may influence the conformation and subsequently the activity of incorporated proteins (Huang, 1986; Helfrich and Jakobsson, 1990; Nielsen et al., 1998).

The phospholipid composition of biological membranes is specific and tightly controlled. The phospholipid content has been catalogued for many different organisms and tissues (Holub et al., 1970; Nozawa et al., 1975; Ray et al., 1969) and comprehensively reviewed by Ansell et al. (1973). In experiments of Wieslander et al. (1986) *Acholeplasma laidlawii* were shown to adjust their lipid composition in response to the incorporation of foreign molecules. They demonstrate an apparent requirement for lipids with a variety of effective shapes. The H_{II} phase, while not found in a physiological setting, provides a means to measure the curvature energy of non-bilayer-prone lipids.

The effects of acyl chain length and unsaturation on the phase transitions of PEs have been characterized (Lewis et al., 1989). The length of the acyl chains has a more profound effect than unsaturation on the phases formed and their transition temperatures, where 16 or more carbons are required for PEs to form the H_{II} phase. DAGs are known to induce the L_{α}-H_{II} phase transition in PCs (Das and Rand, 1986). Complete phase diagrams of DAGs in PCs with similar acyl chain compositions have been constructed (Heimburg et al., 1992; Jimenez-Monreal et al., 1998; Lopez-Garcia et al., 1994).

The present research examines the effects of different acyl chain lengths and saturation levels on monolayer curvature for mixtures of DAGs and PCs. Structural parameters and apparent spontaneous curvatures of two DAGs with extremes of chain length were measured. The induction of the H_{II} phase by dioleoylglycerol (DOG) was analyzed in various PCs with symmetric and asymmetric acyl chains. These results provide a quantitative measure of how different acyl chains of DAG and surrounding phospholipids affect the curvature energy of bilayer membranes.

MATERIALS AND METHODS

Sample preparation

All PCs and DAGs were purchased from Avanti Polar Lipids (Birmingham, AL) and used without further purification. Tetradecane (td) was purchased from Sigma Chemical Co. (St. Louis, MO). Before use, the PCs and DAGs were stored under nitrogen at −18°C.

Appropriate proportions of solid DAG and PC were combined by dry weight, whereas appropriate amounts of the liquid DOG were added from a stock chloroform solution. The lipids were mixed by dissolution in chloroform. The solvent was then removed by rotary evaporation and desiccation under vacuum for a minimum of 1 h. The addition of alkane reduces hydrocarbon packing stress by filling interstices as indicated in Fig. 1, reducing the free energy of the system and allowing the monolayers to curl to their spontaneous curvature (Kirk et al., 1984). Therefore, tetradecane was added to the dry lipid mixtures to make up 16% of the dry weight and equilibrated for 72 h. Double-distilled water was then added to the dry samples by weight and allowed to equilibrate for a minimum of 72 h. This sequence is important to obtain homogeneous samples. Teflon shavings were subsequently added to each sample as an x-ray calibration standard and the samples sealed within an x-ray sample holder between mica windows 1 mm apart. Much of the sample preparation was as described in Chen and Rand (1997, 1998), Leikin et al. (1996), and Rand and Fuller (1994).

X-ray diffraction

The structures of the lipid phases were analyzed using x-ray diffraction, as previously described (Chen and Rand, 1997, 1998; Leikin et al., 1996; Rand and Fuller, 1994). A Rigaku rotating anode x-ray generator produced a $CuK_{\alpha 1}$ line with a wavelength of 1.540 Å that was isolated using a bent quartz crystal monochromator. Guinier x-ray cameras were used to capture the diffraction patterns photographically. The temperature of each sample was controlled to 22 ± 0.2°C unless otherwise stated, using thermoelectric elements.

X-ray repeat spacings in the ratios of 1, $1/\sqrt{3}$, $1/\sqrt{4}$, $1/\sqrt{7}$, $1/\sqrt{9}$, $1/\sqrt{12}$, etc. characterize the hexagonal phase and measure its lattice dimension d_{hex}. The lamellar phase was characterized by the x-ray repeat spacings in the ratios of 1, 1/2, 1/3, 1/4, etc. giving the lattice dimension d_{lam}. The appearance of two phases was detected when two sets of reflections coexisted. Unless otherwise noted, only single phases were observed.

Data analysis

To determine the apparent spontaneous curvatures and structural parameters of the various lipid systems, the following relationships were used. For

an illustration of the variables, see Fig. 1. An effective molecule is introduced to account for the various components of the system (Chen and Rand, 1997) and is used for several structural calculations. For example, the present work involves a system that is composed of PC, DAG, and td in known proportions. The volume of an effective molecule is described by the following (Leikin et al., 1996):

$$V_l = V_{PC} + xV_{DAG} + yV_{td} \quad (1)$$

where V_{PC} = 1305 Å^3, V_{DCG} = 752 Å^3, V_{DOG} = 1114 Å^3, and V_{td} = 156 Å^3; x is the molar ratio of DAG to PC, and y is the molar ratio of td to PC (Chen and Rand, 1997).

The radius of the Luzzati surface or water-polar group interface (R_w) can be determined using the measured hexagonal lattice spacing d_{hex} and water volume fraction (ϕ_w) in the following relationship:

$$R_w = d_{hex}\sqrt{\frac{2\phi_w}{\pi\sqrt{3}}} \quad (2)$$

The area per effective molecule at the Luzzati plane can be determined by:

$$A_w = \frac{2\phi_w V_l}{(1-\phi_w)R_w} \quad (3)$$

To determine whether a system has a well-defined pivotal plane, a normalized diagnostic equation is used (Leikin et al., 1996):

$$\frac{A_w^2}{V_l^2} = \frac{A_p^2}{V_l^2} - \left(\frac{2V_p}{V_l}\frac{A_w}{V_l R_w}\right) \quad (4)$$

If a plot of $(A_w/V_l)^2$ vs. A_w/V_lR_w is linear, then there is a well-defined pivotal plane at V_p/V_l.

The area at the pivotal plane is:

$$A_p = A_w\sqrt{1 + \frac{1-\phi_w}{\phi_w}\frac{V_p}{V_l}} \quad (5)$$

The radius at the pivotal plane is:

$$R_p = R_w\sqrt{1 + \frac{1-\phi_w}{\phi_w}\frac{V_p}{V_l}} \quad (6)$$

$(1/R_{0p})$ is the spontaneous curvature of the mixed lipid monolayer. If $1/R_{0p}$ is a linear function of the mole fractions of the components, the apparent spontaneous curvature of each lipid, $1/R_{0p}{}^{PC}$ for PC and $1/R_{0p}{}^{DAG}$ for DAG, can be determined.

$$\frac{1}{R_{0_p}} = (1-m_{DAG})\frac{1}{R_{0_p}^{PC}} + (m_{DAG})\frac{1}{R_{0_p}^{DAG}} \quad (7)$$

where m_{DAG} is the mole fraction of DAG and is given by:

$$m_{DAG} = x/(1+x) \quad (8)$$

and x is the mole ratio of DAG to PC.

RESULTS

Apparent spontaneous curvatures of DCG and DOG

A preliminary experiment was performed to determine whether there was a difference in the structural parameters of the H_{II} phases induced by dicaprylglycerol (DCG) and DOG in dioleoylphosphatidylcholine (DOPC). As the mole fraction of either DAG increased, the lattice dimensions decreased, indicating increased negative curvature of the monolayers. The hexagonal lattice dimensions d_{hex} are plotted against mole fractions DCG/DOPC and DOG/DOPC (Fig. 2). The systems show parallel, linear relationships between d_{hex} and DAG content. The lattice dimensions for the DCG system are larger than the DOG system.

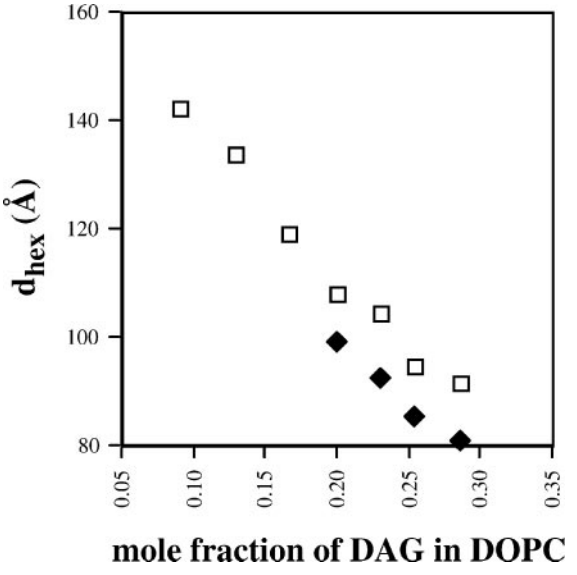

FIGURE 2 Plot comparing the equilibrium d_{hex} spacings, in excess water and with tetradecane, for various mole fractions of (□) DCG in DOPC and (◆) DOG in DOPC.

Phase diagrams were constructed for various compositions of DCG in DOPC (Fig. 3 *A*) and DOG in DOPC (Fig. 3 *B*). The lattice dimensions, d_{hex}, were plotted over a hydration range for each DAG composition. At full hydration, the points were averaged and fitted with a horizontal line. Because there was no detectable difference in dimension for samples of equal water content but different DAG compositions at less than full hydration, all of the data derived from dehydrated samples, within each DAG, were pooled and fitted with a common second-order polynomial (Fig. 3, *A* and *B*).

The weight fraction of water (1-c) at full hydration was calculated by the intersection of the horizontal line and a second-order polynomial curve for each phase diagram, and is shown in Tables 1 and 2. The dimensions of dehydrated samples for each phase diagram (Fig. 3) were used to calculate several structural parameters which were then used in the diagnostic equation (Eq. 4).

The linearity of the diagnostic plots indicate well-defined pivotal planes. The positions of the pivotal planes (V_p/V_l) for both DCG and DOG in DOPC, given by the slopes in Fig. 4, *A* and *B* were observed to be insignificantly different. Several other structural parameters, as shown in Fig. 1, were calculated for the system at full hydration and are shown in Tables 1 and 2.

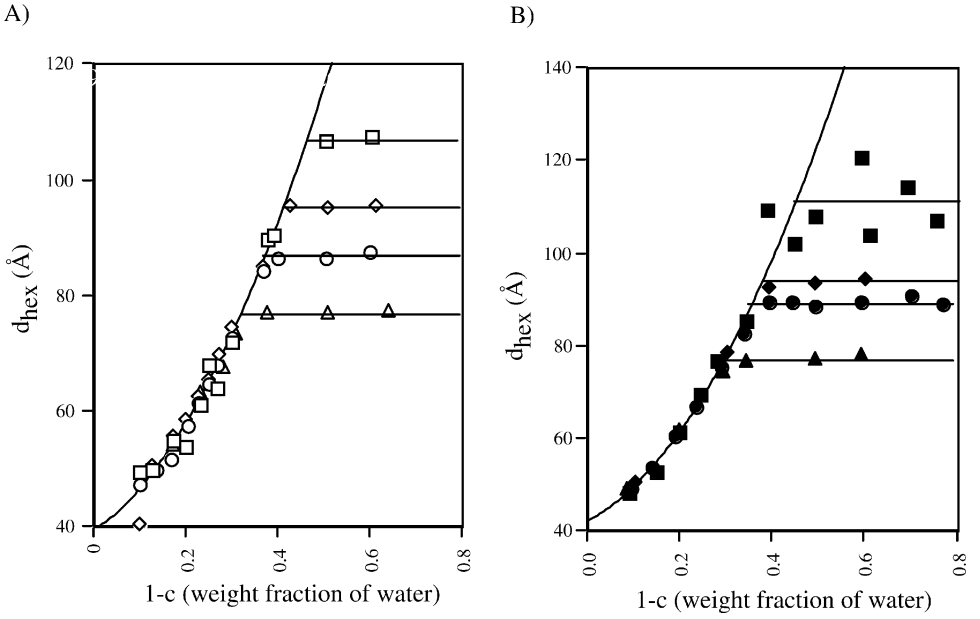

FIGURE 3 Lattice dimensions, d_{hex}, as they vary with the water content for different mole fractions of (*A*) DCG in DOPC: □, 20; ◇, 25; ○, 30; and △, 35 mol%; (*B*) DOG in DOPC: ■, 17; ◆, 20; ●, 24; and ▲, 29 mol%.

In both the DCG and DOG systems the effective molecular areas at the polar group/water interface are similar and remain fairly constant as DAG content increases. However, the molecular areas at the pivotal plane appear greater in the DOG system (Fig. 5 *A*) for the same mole fraction. Fig. 5 *B* shows that the interaxial bilayer thickness and the associated hydrocarbon thickness are slightly, but consistently, greater in the DOG system. These thicknesses increase with increasing mole fraction DOG in DOPC, whereas they remain fairly constant for DCG in DOPC.

The radius of spontaneous curvature can be calculated from Eq. 6, using the equilibrium hydration values of Tables 1 and 2, and V_p/V_l, determined from Fig. 4, *A* and *B*. The spontaneous curvatures are plotted against the DAG mole fraction in Fig. 6 and are used to determine the apparent spontaneous curvatures of the individual components, which are shown in Table 3.

H_{II} phase induction of PCs by DOG

The ability of DOG to induce the H_{II} phase transition in PCs of different acyl chain composition, in the presence of tetradecane, was measured and is summarized in Fig. 7. Symmetrical PCs with two saturated acyl chains 10–18 carbons long were not induced to form the H_{II} phase by 25 mol % DOG, even up to 60°C. Symmetrical PCs with two monounsaturated acyl chains 14–18 carbons long were induced to form a single H_{II} phase by 25 mol % DOG at 22°C. Asymmetrical PCs all showed the presence of an H_{II} phase at 22°C. DOG induced 1-palmitoyl, 2-oleoyl phosphatidyl-

TABLE 1 Structural parameters of the fully hydrated reverse hexagonal phase for various molar fractions of DCG in DOPC (see Fig. 1 for the parameters)

m_{DCG}	d_{hex} (Å)	1-c	V_l (Å^3)	A_w (Å^2)	A_p (Å^2)	A_t (Å^2)	R_w (Å)	R_p (Å)	d_l (Å)	d_m (Å)	d_{lhc} (Å)
0.20	107	0.465	1861	70.0	78.1	110	43.5	48.5	36.5	55.6	26.2
0.25	95	0.418	1937	71.4	81.3	118	36.5	41.6	36.6	53.6	26.6
0.30	87	0.368	2025	70.8	84.6	125	31.1	37.2	37.6	53.1	27.6
0.35	77	0.321	2125	75.6	92.5	140	26.4	32.3	36.1	49.9	26.8

TABLE 2 Structural parameters of the fully hydrated reverse hexagonal phase for various molar fractions of DOG in DOPC (see Fig. 1 for the parameters)

m_{DOG}	d_{hex} (Å)	1-c	V_l (Å^3)	A_w (Å^2)	A_p (Å^2)	A_t (Å^2)	R_w (Å)	R_p (Å)	d_l (Å)	d_m (Å)	d_{lhc} (Å)
0.17	106	0.470	1889	73.4	83.6	114	43.2	48.1	35.4	54.2	25.5
0.20	95	0.408	1946	70.4	82.8	118	36.0	41.1	37.1	54.0	27.0
0.24	90	0.380	2036	71.6	85.7	124	32.8	38.1	37.7	53.7	27.7
0.29	78	0.310	2149	70.7	89.2	136	25.7	31.2	38.4	52.2	28.5

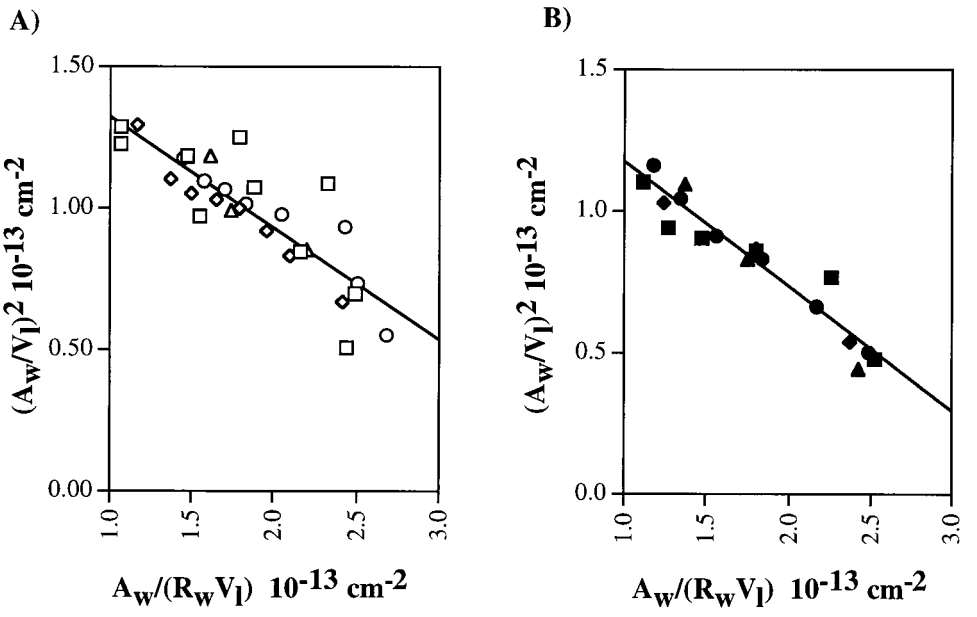

FIGURE 4 Diagnostic plots for (*A*) DCG in DOPC with the data derived from □, 20; ◇, 25; ○, 30; and △, 35 mol % DCG; (*B*) DOG in DOPC with the data derived from ■, 17; ◆, 20; ●, 24; and ▲, 29 mol % DOG. Data for each lipid were combined and fitted by Eq. 4 (see text) to give the following: $A_w^2/V_l^2 = 1.721 - [0.394(A_w/V_lR_w)]$ for DCG, and $A_w^2/V^2 = 1.612 - [0.439(A_w/V_lR_w)]$ for DOG. The slope of each line gives the pivotal plane position V_p/V_l.

choline (POPC) and 1-steroyl,2-oleoyl phosphatidylcholine (SOPC) to form an H_{II} phase in equilibrium with a liquid-crystalline lamellar phase (L_α) at 22°C, but a pure H_{II} phase at 50°C.

DISCUSSION

The objective of this work was to measure the ability of different DAGs to induce negative curvature in various PCs and to measure their apparent spontaneous curvatures. Using two extremes of DAG, in DOPC, R_{0p}^{DCG} was determined to be −13.3 Å and R_{0p}^{DOG} was determined to be −10.1 Å. R_{0p}^{DOG} measured in DOPE was −11.5 Å (Leikin et al., 1996). Increased hydrophobic volume below the pivotal plane is the likely cause of increased negative spontaneous curvature. The unsaturated and longer acyl chains of DOG contribute considerably more hydrophobic volume

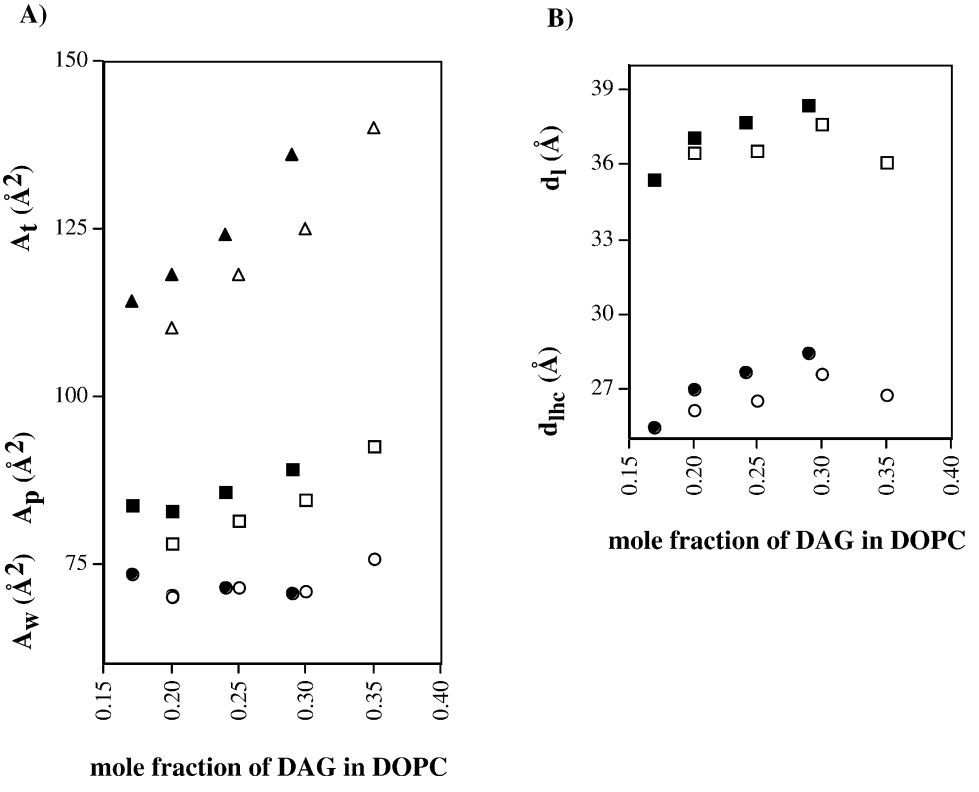

FIGURE 5 Structural parameters (see Fig. 1) derived for the equilibrium hydration condition comparing the DCG (*open symbols*) and DOG (*solid symbols*) systems in DOPC as they vary with mole fraction DAG. (*A*) Molecular areas at the polar group/water interface and at the pivotal plane; (*B*) the interaxial effective bilayer thickness and interaxial hydrocarbon thickness, as defined in Fig. 1 *B*.

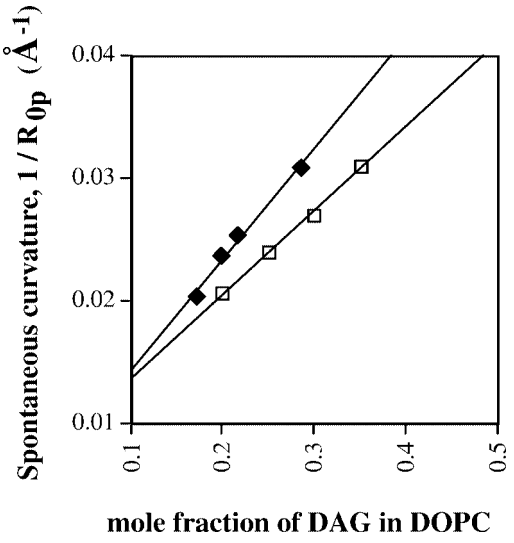

FIGURE 6 Plots of spontaneous curvature for mixtures of (□) DCG and (♦) DOG in DOPC. Least-square linear fits are $1/R_{0p}{}^{DCG} = 0.068\ m_{DCG} + 0.007$ and $1/R_{0p}{}^{DOG} = 0.094\ m_{DOG} + 0.005$.

per molecule than does DCG. One might have expected a bigger difference between DAGs with chain lengths that differ by nearly a factor of two, and where the longer chains are unsaturated.

TABLE 3 The apparent spontaneous curvatures of DCG, DOG, and DOPC determined from the slopes and intercepts in Fig. 6

Lipid	Apparent Spontaneous Curvature $1/R_0$ ($Å^{-1}$)	Apparent Spontaneous Radius of Curvature R_0 (Å)
DCG	−0.075	−13.3
DOG	−0.099	−10.1
DOPC	−0.005 to −0.007	−143 to −200

Using a two-sample *t*-test, the apparent spontaneous curvatures of DCG and DOG are significantly different ($p < 0.05$).

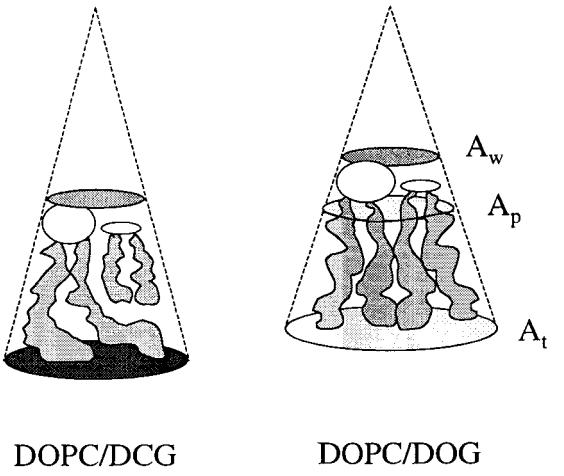

FIGURE 8 Schematic representation of the structural differences between DCG/DOPC mixtures and DOG/DOPC mixtures.

Fig. 8 schematically summarizes the structural differences between these two systems. The DCG molecules have shorter acyl chains (10 carbons) than the surrounding DOPC molecules (18 carbons). Depending on the disposition of the polar groups, space at the ends of the DCG chains is likely filled by the longer chains of DOPC. In the DOG system the acyl chains are the same length, so that the DOPC chains are not required to fill such space, and on a molar basis DOG contributes a greater hydrocarbon volume.

Effective molecules of both the DCG and DOG systems had the same molecular area at the Luzzati plane, i.e., at the polar group/water interface, A_w (Fig. 8). However, the molecular areas at the pivotal planes (A_p) and at the chain terminals (A_t) of the DOG system are larger than those of the effective molecules in the DCG system. The interaxial bilayer thickness (d_l) and hydrocarbon thickness (d_{lhc}) are

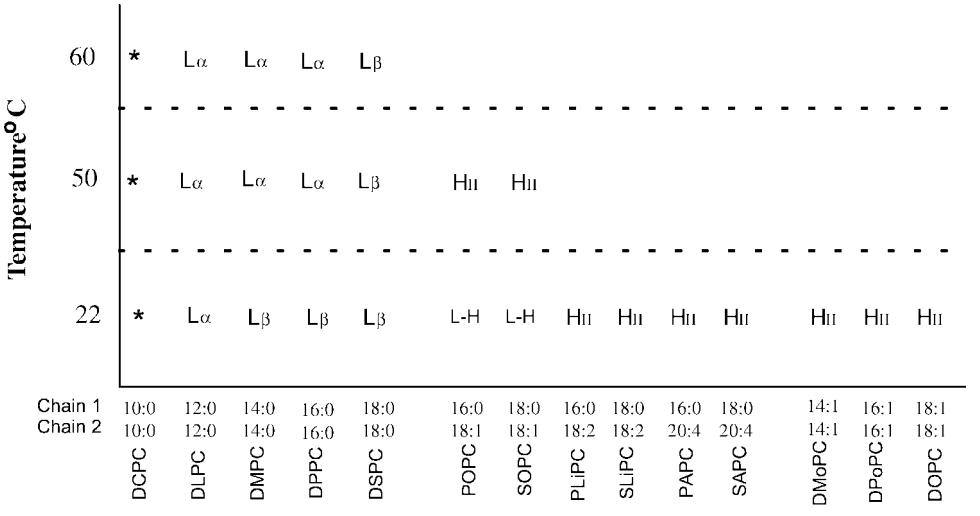

FIGURE 7 Phases formed by lipid assemblies composed of 25 mol % DOG in PCs of indicated acyl chain composition in the presence of 16 wt % tetradecane in excess water. *, a disordered phase; L_α, the liquid-crystalline lamellar phase; L_β, the gel lamellar phase; H_{II}, the reverse hexagonal phase; L-H, a coexistence of the L_α and H_{II} phases.

larger, and perhaps increase faster with DAG content, in the H_{II} phase induced by DOG compared with that induced by DCG.

Decreasing the ratio of the volumes above and below the pivotal plane of an effective molecule is the likely cause of increased negative spontaneous curvature. In this study we added DOG to PCs with a variety of hydrocarbon chains. The addition of 16 wt % tetradecane, which does not change spontaneous curvature (Chen and Rand, 1997), should allow the mixtures to form hexagonal phases even of very large dimension or low spontaneous curvature (Rand et al., 1990). For the H_{II} phase to form the combined curvature contributions of PC and DOG must reach a critical value, lowering the hexagonal phase free energy. Phospholipid chain unsaturation appears to be very important in lowering that free energy. PCs with saturated acyl chains are not induced to form the H_{II} phase by 25 mol % DOG at all, even at 60°C. Some degree of unsaturation, described by Fig. 7, appears to be required for even 25 mol % DOG to induce the H_{II} phase in these PCs.

Complete phase diagrams have been constructed by others for 1,2-dimyristoylglycerol (DMG) in 1,2-dimyristoylphosphatidylcholine (DMPC), 1,2-dipalmitoylglycerol (DPG) in 1,2-dipalmitoylphosphatidylcholine (DPPC), and 1-palmitoyl, 2-oleoyl glycerol (POG) in POPC (Heimburg et al., 1992; Lopez-Garcia et al., 1994; Jimenez-Monreal et al., 1998), respectively. For the di-saturated DMG in DMPC, the results show that the H_{II} phase appears at 45 mol %, above 50°C. The phase diagram constructed for the di-saturated DPG in DPPC shows the coexistence of the H_{II} phase with the L_α and an isotropic phase at compositions $>$40 mol % above 60°C. In the phase diagram of POG in POPC the H_{II} phase does not form, but rather a cubic phase forms, which also has an overall negative curvature. It should be noted that a hydrocarbon, such as tetradecane, was not used in that study. Therefore, hexagonal phases of large dimension could not form and any predisposition to form structures of small curvature would not be detected.

By whatever mechanism, membranes are differentially perturbed by different DAGs of different acyl chain lengths and degrees of unsaturation (Goldberg and Zidovetzki, 1997). For example, DAGs with unsaturated chains or short, saturated chains have been shown to activate PKC, whereas DAGs with long, saturated chains do not (references within Goldberg and Zidovetzki, 1997).

Membrane fusion is a process that has been suggested to exploit lipid curvature energy when forming highly curved structural intermediates (Chernomordik et al., 1985). The various DAGs may provide an elaborate arsenal of building blocks to custom fit the fusion intermediate structures with lipids of the required curvature in the appropriate local phospholipid medium. This suggestion implies that various DAGs fine-tune different aspects of the formation of these highly curved intermediates. For instance, the rate of intermediate transition (i.e., stalk intermediate to hemifusion intermediate) may be controlled by the presence of DAGs with different curvatures.

We acknowledge the support of the Natural Sciences and Engineering Research Council of Canada.

REFERENCES

Ansell, G. B., J. N. Hawthorne, and R. M. C. Dawson, eds. 1973. Form and Function of Phospholipids. Elsevier Scientific Publishing Company, New York.

Bolen, E. J., and J. J. Sando. 1992. Effect of phospholipid unsaturation on protein kinase C activation. *Biochemistry.* 31:5945–5951.

Chen, Z., and R. P. Rand. 1997. The influence of cholesterol on phospholipid membrane curvature and bending elasticity. *Biophys. J.* 73: 267–276.

Chen, Z., and R. P. Rand. 1998. Comparative study of the effects of several n-alkanes on phospholipid hexagonal phases. *Biophys. J.* 74:944–952.

Chernomordik, L. V., M. M. Kozlov, G. B. Melikyan, I. G. Abidor, V. S. Markin, and Y. A. Chizmadzhev. 1985. The shape of lipid molecules and monolayer membrane fusion. *Biochim. Biophys. Acta.* 812:643–655.

Chernomordik, L., M. M. Kozlov, and J. Zimmerberg. 1995. Lipids in biological membrane fusion. *J. Membr. Biol.* 146:1–14.

Cullis, P. R., and B. de Kruijff. 1979. Lipid polymorphism and the functional roles of lipids in biological membranes. *Biochim. Biophys. Acta.* 559:399–420.

Das, S., and R. P. Rand. 1986. Modification by diacylglycerol of the structure and interaction of various phospholipid bilayer membranes. *Biochemistry.* 25:2882–2889.

Epand, R. M., ed. 1997. Lipid Polymorphism and Membrane Properties. Academic Press, San Diego.

Go, M., K. Sekiguchi, H. Nomura, U. Kikkawa, and Y. Nishizuka. 1987. Further studies on the specificity of diacylglycerol for protein kinase C activation. *Biochem. Biophys. Res. Commun.* 144:598–605.

Goldberg, E. M., and R. Zidovetzki. 1997. Effects of dipalmitoylglycerol and fatty acids on membrane structure and protein kinase C activity. *Biophys. J.* 73:2603–2614.

Gruner, S. M. 1985. Intrinsic curvature hypothesis for biomembrane lipid composition: a role for nonbilayer lipids. *Proc. Natl. Acad. Sci. U.S.A.* 82:3665–3669.

Heimburg, T., U. Wurz, and D. Marsh. 1992. Binary phase diagram of hydrated dimyristoylglycerol-dimyristoylphosphatidylcholine mixtures. *Biophys. J.* 63:1369–1378.

Helfrich, W. 1973. Elastic properties of lipid bilayers: theory and possible experiments. *Z. Naturforsch.* 28C:693–703.

Helfrich, P., and E. Jakobsson. 1990. Calculation of deformation energies and conformations in lipid membranes containing gramicidin channels. *Biophys. J.* 57:1075–1084.

Holub, B. J., A. Kuksis, and W. Thompson. 1970. Molecular species of mono-, di-, and triphosphoinositides of bovine brain. *J. Lipid Res.* 11:558–564.

Huang, H. W. 1986. Deformation free energy of bilayer membrane and its effect on gramicidin channel lifetime. *Biophys. J.* 50:1061–1070.

Jimenez-Monreal, A. M., J. Villalain, F. J. Aranda, and J. C. Gomez-Fernandez. 1998. The phase behavior of aqueous dispersions of unsaturated mixtures of diacylglycerols and phospholipids. *Biochim. Biophys. Acta.* 1373:209–219.

Kirk, G. L., S. M. Gruner, and D. L. Stein. 1984. A thermodynamic model of the lamellar to inverse hexagonal phase transition of lipid membrane-water system. *Biochemistry.* 23:1093–1102.

Leikin, S., M. M. Kozlov, N. L. Fuller, and R. P. Rand. 1996. Measured effects of diacylglycerol on structural and elastic properties of phospholipid membranes. *Biophys. J.* 71:2623–2632.

Lewis, R. N., D. A. Mannock, R. N. McElhaney, D. C. Turner, and S. M. Gruner. 1989. Effect of fatty acyl chain length and structure on the

lamellar gel to liquid-crystalline and lamellar to reversed hexagonal phase transitions of aqueous phosphatidylethanolamine dispersions. *Biochemistry.* 28:541–548.

Lopez-Garcia, F., J. Villalain, J. C. Gomez-Fernandez, and P. J. Quinn. 1994. The phase behavior of mixed aqueous dispersions of dipalmitoyl derivatives of phosphatidylcholine and diacylglycerol. *Biophys. J.* 66: 1991–2004.

Luzzati, V., and F. Husson. 1962. The structure of the liquid-crystalline phases of lipid-water systems. *J. Cell. Biol.* 12:207–219.

Marignani, P. A., R. M. Epand, and R. J. Sebaldt. 1996. Acyl chain dependence of diacylglycerol activation of protein kinase C activity in vitro. *Biochem. Biophys. Res. Commun.* 225:469–473.

Mori, T., Y. Takai, B. Yu, J. Takahashi, Y. Nishizuka, and T. Fujikura. 1982. Specificity of the fatty acyl moieties of diacylglycerol for the activation of calcium-activated, phospholipid-dependent protein kinase. *J. Biochem.* 91:427–431.

Nielsen, C., M. Goulian, and O. S. Andersen. 1998. Energetics of inclusion-induced bilayer deformations. *Biophys. J.* 74:1966–1983.

Nishizuka, Y. 1984. The role of protein kinase C in cell surface signal transduction and tumour promotion. *Nature.* 308:693–698.

Nozawa, Y., H. Fukushima, and H. Iida. 1975. Studies on *Tetrahymena* membranes: modification of surface membrane lipids by replacement of tetrahymenol by exogenous ergosterol in *Tetrahymena pyriformis. Biochim. Biophys. Acta.* 406:248–263.

Ortiz, A., F. J. Aranda, J. Villalain, C. San Martin, V. Micol, and J. C. Gomez-Fernandez. 1992. 1,2-Dioleoylglycerol promotes calcium-induced fusion in phospholipid vesicles. *Chem. Phys. Lipids.* 62: 215–224.

Rand, R. P., and N. L. Fuller. 1994. Structural dimensions and their changes in a reentrant hexagonal-lamellar transition of phospholipids. *Biophys. J.* 66:2127–2138.

Rand, R. P., N. L. Fuller, S. M. Gruner, and V. A. Parsegian. 1990. Membrane curvature, lipid segregation, and structural transitions for phospholipids under dual-solvent stress. *Biochemistry.* 29:76–87.

Ray, T. K., V. P. Skipski, M. Barclay, E. Essner, and F. M. Archibald. 1969. Lipid composition of rat liver plasma membranes. *J. Biol. Chem.* 244:5528–5536.

Roos, D. S., and P. W. Choppin. 1985a. Biochemical studies on cell fusion. I. Lipid composition of fusion-resistant cells. *J. Cell Biol.* 101: 1578–1590.

Roos, D. S., and P. W. Choppin. 1985b. Biochemical studies on cell fusion. II. Control of fusion response by lipid alteration. *J. Cell Biol.* 101: 1591–1598.

Rothman, J. E., and J. Lenard. 1977. Membrane asymmetry. The nature of membrane asymmetry provides clues to the puzzle of how membranes are assembled. *Science.* 195:743–753.

Siegel, D. P., J. Banschbach, D. Alford, H. Ellens, L. J. Lis, P. J. Quinn, P. L. Yeagle, and J. Bentz. 1989. Physiological levels of diacylglycerols in phospholipid membranes induce membrane fusion and stabilize inverted phases. *Biochemistry.* 28:3703–3709.

Verkleij, A. J., R. F. A. Zwaal, B. Roelofsen, P. Comfurius, D. Kastelijn, and L. L. M. Van Deenen. 1973. The asymmetric distribution of phospholipids in the human red cell membrane. A combined study using phospholipases and freeze-etch electron microscopy. *Biochim. Biophys. Acta.* 323:178–193.

Wieslander, A., L. Rilfors, and G. Lindblom. 1986. Metabolic changes of membrane lipid composition in *Acholeplasma laidlawii* by hydrocarbons, alcohols, and detergents: arguments for effects on lipid packing. *Biochemistry.* 25:7511–7517.